# Using crop fall patterns to provide an insight into thunderstorm downbursts

Sterling, M., Huo, S., and Baker, C.J.

**Abstract**

This paper examines whether crop fall patterns due to thunderstorm downburst-like events can provide an insight into the flow structure of a downburst. To explore this phenomenon, a novel three-dimensional analytical model for the velocity flow field is derived and coupled with a generalised plant model which is capable of modelling crop failure. Through this approach we have established the concept of the lodging front – a dimensionless variable used to quantify the spatial extent of crop failure. Crop failure is shown to result in a diverging pattern and the angles at which the crop falls has been shown to collapse onto a single curve when suitably normalised. Comparison with full-scale data suggests that the model is capable of predicting realistic crop fall patterns and could potentially be used in the future to assess the strength of downbursts.

## Notation

| | |
|---|---|
| a | crop stem radius (m) |
| $AC_F$ | crop drag area (m$^2$) |
| $D$ | minimum duration of downburst (s) |
| $\overline{D}$ | $DU_m/r_m$ |
| $g$ | acceleration due to gravity (m/s$^2$) |
| $r$ | radial distance from downburst impingement (m) |
| $r_1$ | inner edge of lodging area for stationary downburst (m) |
| $r_2$ | outer edge of lodging area for stationary downburst (m) |
| $\bar{r}$ | $r/r_m$ |
| $\bar{r}_1$ | $r_1/r_m$ |
| $\bar{r}_2$ | $r_2/r_m$ |
| $r_m$ | radial distance corresponding to $U_m$ (m) |
| $Q$ | translation speed of the downburst (m/s) |
| $\bar{Q}$ | $Q/U_m$ |
| $t$ | crop stem thickness (m) |
| $U(r,z)$ | radial flow velocity component (m/s) |
| $\overline{U}$ | $U/U_m$ |
| $U_m$ | maximum value of the radial velocity in the downburst (m/s) |
| $U_{mc}$ | maximum value of the radial velocity at crop height (m/s) |
| $W(r,z)$ | vertical velocity component (m/s) |
| $\overline{W}$ | $W/U_m$ |
| $X$ | centre of gravity of the plant above the ground (m) |
| $x$ | distance from downburst centre in direction of storm translation |
| $\bar{x}$ | $x/r_m$ |
| $y$ | distance from downburst centre normal to direction of storm translation |
| $\bar{y}$ | $y/r_m$ |
| $z$ | vertical distance above the ground (m) |
| $z_m$ | vertical distance corresponding to $U_m$ (m) |
| $\bar{z}$ | $z/z_m$ |
| | |
| $\alpha$ | wind angle relative to *x* axis |
| $\delta$ | $z_{max}/r_{max}$ |
| $\theta$ | crop fall direction relative to *x* axis |
| $\rho$ | density of air (kg/m$^3$) |
| $\omega_n^2$ | radial natural frequency of the plant (rad/s) |
| $\Omega$ | resultant wind speed (m/s) |
| $\overline{\Omega}$ | $\Omega/U_m$ |
| $\Omega_l$ | crop lodging velocity (m/s) |
| $\overline{\Omega_l}$ | $\Omega_l/U_{mc}$ |

## 1. Background

Interest in tornadoes and thunderstorm downbursts has continued to grow within the wind engineering community. These types of transient winds are complex and, at this present moment in time, the community is still considering how best they can be addressed in the design process. Whilst there are still no formal rules for how such events can be best simulated, peer reviewed commentary has appeared in ASCE 49-21 (2021) which outlines the main parameters which need be considered and highlights many of the existing knowledge gaps. These considerable knowledge gaps have encouraged many to undertake research in this area. With respect to downbursts, numerous attempts to physically simulate such events have been undertaken (e.g., Chay and Letchford, 2002a; Chay and Letchford, 2002b; Babaei et al., 2021; Jesson et al., 2015; Mason et al., 2009; McConville et al., 2009; Romanic and Hangan, 2020), in addition to numerical modelling (e.g., Aboshosha et al., 2015; Kim and Hangan, 2007; Li et al., 2012) to name but a few.

What has tended to hamper progress is the complexity of the geometric, kinematic and dynamic scaling that must be achieved (ASCE 49-21, 2021; Baker and Sterling, 2019; Romanic et al., 2020). Thus, whilst general trends can be inferred, it is often difficult to compare the results between different simulations and thus meaningfully extrapolate the findings for the purposes of design. Furthermore, relative to boundary layer winds, there is lack of comprehensive full-scale data available, although the work undertaken by Solari et al. (Burlando et al., 2018; Canepa et al., 2020; Solari et al; 2015a,b; Solari et al., 2020) are noticeable exceptions. Often the classic work of Fujitia (1981) and Hjelmelft (1988) are referenced, which whilst informative, do not have sufficient resolution close to the ground to be of interest for a variety of applications.

Several analytical models have been developed (Abd-Elaal et., 2013; Chay et al., 2006; Holmes and Oliver, 2000; Ivan, 1986; Jesson and Sterling, 2017) which either have some basis in physics or are simply useful empirical fits to the data. A case has even been put forward to suggest that the approach adopted to date perhaps may be overcomplicating the issue (Jesson et al., 2019). Notwithstanding the research in this area, we still know relatively little about downbursts compared to either boundary layer winds or even tornadoes. This is perhaps not too surprising given that downbursts tend to be highly localised in both space and time. Hence, it would be beneficial to find an alternative approach which could provide an insight into downbursts, particularly near the ground. With this in mind, it is hypothesised that crop fall patterns may potentially provide an alternative mechanism in which to understand downbursts and it is with this issue that the paper is concerned.

Multidisciplinary work undertaken by the authors (Baker et al., 2014; Berry et al., 2003; Berry et al., 2004; Sterling et al., 2003) on wind induced crop fall have indicated that not only is it possible to back calculate the wind speed but also inform husbandry decisions and thus save a considerable amount of money – Berry (2022) suggests that in the UK alone, this research has resulted in savings to the farming industry of ~£2-3M p.a. A description of the model developed by the authors can be found in Baker et al. (2014) and is briefly outlined in what follows for the benefit of the reader. By coupling this model with a new analytical model to represent the flow field of a downburst-like event, this paper explores the crop fall patterns that may arise due to these transient wind events.

The paper is organised as follows: section 2 presents details relating to the crop model and relevant crop parameters which are used later in the paper. Section 3 introduces a new downburst model by building on the work of Baker and Sterling (2017). Section 4 combines the work of sections 2 and 3 and explores crop fall patterns which occur as a result of a variety of downburst events. Finally, appropriate conclusions are presented in section 5.

## 2. Crop Modelling

This section briefly outlines the generalised crop fall model developed by Baker et al. (2014) since it is key to understanding the focus of the paper. The crops are essentially modelled as a series of inextensible cantilevers with a wind load (mean + fluctuating) applied at the free end. The fixed end of the cantilever represents the plant's foundations, i.e., the root-soil interaction. The bending moment arising from the wind action can then be calculated along the stem (cantilever). The resultant moment is then compared to the plant's ability to resist bending which is represented by two separate failure models – the first model accounting for stem resistance and the second accounting for root resistance, both of which are essentially functions of various plant and soil parameters. When the applied bending moment due to the wind is equal to or exceeds the plant's failure moment – crop fall (often referred to as 'lodging') is known to occur, i.e., the plant undergoes a permanent displacement from the vertical. This results in either immediate failure, failure due to disease or increased costs at harvest time. Considerable work has been undertaken to ensure that the effects of this are minimised for boundary layer winds (Berry et al., 2003; Berry et al., 2004; Berry et al., 2020; Joseph et al., 2020; Mohammadi et al., 2020). Recently the impact of tornados on crops and trees has started to receive increased attention (Baker et al., 2020; Lombardo et al., 2015; Rhee and Lombardo, 2018) the results of which has led to an increased understanding tornado dynamics. However, to the best of the author's knowledge, the failure of crops due to downburst type events has not received significant attention beyond the initial work of Fujitia (1981).

The crop model accounts for both single (non-interlocking) and interlocking plants. There are similarities with the approach adopted for dynamic structures in that the stochastic nature of the wind is considered by reference to the wind spectrum. This enables two failure velocities to be obtained - one for the stem ($\Omega_l$) and one for the root. In the current paper we will not consider the latter since it is assumed that the timescale over which the downburst occurs is insufficient to cause failure in the roots, since root failure is typically a function of fatigue. Stem failure however occurs relatively instantaneously, i.e., it is essentially associated with a short-term wind gust.

The model essentially applies Newton's second law to the top of the canopy and by considering the fluctuating wind load, an expression for the bending moment at any point along the stem is derived. Using this model in conjunction with the standard theory of bending, it is possible to derive (after much manipulation) the following expression for stem failure wind speed $\Omega_l$ measured at the height of the plant centre of gravity. The model formulated by Baker et al. (2014) is expressed as follows:

$$\Omega_l = \left( \frac{\omega_n^2 (z_c/g)(\sigma \pi a^3/4)\left(1-((a-t)/a)^4\right)}{\left(1+\omega_n^2 (X/g)\right)(0.5\rho \mathrm{A}C_F)} \right)^{0.5} \tag{1}$$

where $\omega_n$ is the radial natural frequency of the plant, $z_c$ is the centre of gravity of the plant above the ground, $g$ is the acceleration due to gravity, $\sigma$ is the stem strength, $a$ is the stem radius, $X$ is the height of the centre of mass of the crop canopy, $t$ is the stem thickness, $\rho$ is the density of air and $\mathrm{A}C_F$ is the plant's drag area.

As noted above, the authors have undertaken considerable work in this area which has enabled them to obtain a variety of appropriate plant parameters for different crops. Table one outlines such parameters for maize measured in the UK. These values will be used in what follows (although it is acknowledged that depending on the variety of maize and corresponding husbandry treatments, these values could vary considerably).

**Table 1.** Crop parameters for maize (from Berry et al., 2020).

| Parameter | Mean | Standard deviation |
|---|---|---|
| $\omega_n$ (Hz) | 4.4 | 0.75 |
| $z_c$ (m) | 0.95 | 0.1 |
| $\sigma$ (mPa) | 21.9 | 4 |
| $a$ (m) | 0.013 | 0.0013 |
| $t$ (m) | 0.0026 | 0.0005 |
| $\mathrm{A}C_F$ ($m^2$) | 0.153 | 0.02 |

On the assumption that all the above parameters are normally distributed, an array of random plant characteristics using the above parameters can be generated. These can then be used to calculate appropriate lodging wind speeds for each plant. This was found to have a mean of 11.95 m/s with a standard deviation of 2.22 m/s and thus a ratio of standard deviation to mean of 0.186.

## 3. Downburst wind field modelling

The transient nature of a downburst ensures that the corresponding flow field is complex and varies both in time and space (Solari et al., 2015a). Traditionally, the flow field has been considered akin to that of an impinging jet (Hjelmet, 1988) as illustrated in Figure 1. However, this figure is an idealised schematic of what a downburst could look like at one moment in time. Each downburst is different (Jesson et al., 2019) and as such the idealised image shown in Figure 1, may not be an appropriate representation of the event throughout its lifecycle. Nevertheless, such an image has so far stood the test of time and provides a useful framework to formulate downburst models.

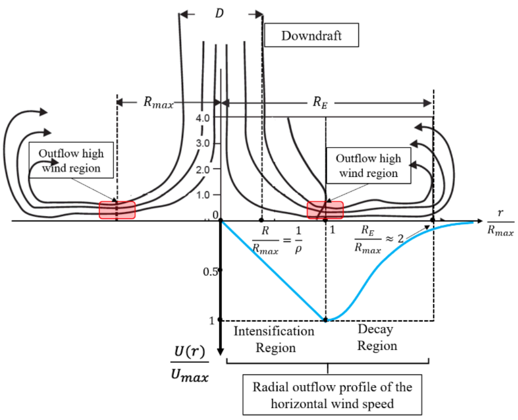


**Figure 1.** Idealised schematic of a downburst Xhelaj et al. (2020) (Adapted from Hjelmelft, 1988).

Xhelaj et al. (2020) adapted Hjelmfelt's classic schematic (Hjelmelft, 1988) to help visualise the variation of radial outflow from the impingement centre to the edge of the gust front (Figure 1). To account for the change in flow field with respect to time, Xhelaj et al. (2020) expressed the distribution of radial velocity as a combination of a radial flow component and a time decay component. Now, whilst the inclusion of the time decay component was a novel approach, we have chosen to assume in what follows that there is no time variation for several reasons. Firstly, whilst convenient, this is an approximation since different parts of the downburst would have velocity variations at different times. Secondly, there is a discontinuity in radial velocity at the outflow high wind region. Also, the focus of this paper is to provide an insight into potential cropfall patterns that could occur in a downburst-type event rather than simulate the entire lifecycle of a downburst.

In developing a model of a downburst we first assume the following for the radial velocity $U$ as a function of the radial distance from the centre of the impingement $r$, and the vertical distance above ground $z$.

$$\overline{U} = \frac{2\bar{r}}{(1+\bar{r}^2)} \frac{4\bar{z}}{(3+\bar{z}^4)} \qquad (2)$$

Here the normalized radial velocity, radius and height are given by $\overline{U} = U/U_m$, $\bar{r} = r/r_m$ and $\bar{z} = z/z_m$ where $U_m$ is the maximum value of the radial velocity at $r = r_m$ and $z = z_m$. Thus $\overline{U} = 1$ at $\bar{r} = 1$ and $\bar{z} = 1$. Equation (2) is plotted in Figure 2 below and shows the characteristic peak of radial velocity in both the radial and vertical directions. This form is similar to that used by the authors in the past in the analysis of tornadoes (Baker and Sterling, 2017), but the vertical variation has a more rapid fall with height above the ground. This will be seen to be significant in what follows.

The radial continuity equation is as follows, where $W$ is the vertical velocity, and it is assumed there is no circumferential velocity component.

$$\frac{1}{\bar{r}}\frac{\partial(\bar{U}\,\bar{r})}{\partial\bar{r}}+\frac{1}{\delta}\frac{\partial\bar{W}}{\partial\bar{z}}=0 \quad (3)$$

where $\bar{W}=W/U_m$ and $\delta=z_m/r_m$. Using the above expression for $\bar{U}$ leads to the following expression for $\bar{W}$.

$$\bar{W}=-\frac{8\delta}{(1+\bar{r}^2)^2}\frac{\tan^{-1}(\bar{z}/\sqrt{3})}{\sqrt{3}} \quad (4)$$

For large values of $\bar{z}$ the vertical velocity tends towards:

$$\bar{W}=-\frac{8\delta}{(1+\bar{r}^2)^2}\frac{\pi}{2\sqrt{3}} \quad (5)$$

Equation (5) is plotted in Figure 3. The radial variation is similar to that obtained in earlier studies with a downward peak on centre line. In the earlier work $\bar{W}$ was unbound and increased slowly with height in a somewhat unrealistic way, but in the present model the vertical variation now tends to a constant value for large values of $\bar{z}$ (i.e., $\bar{z}/\delta$ =7.23 at the downburst centre).

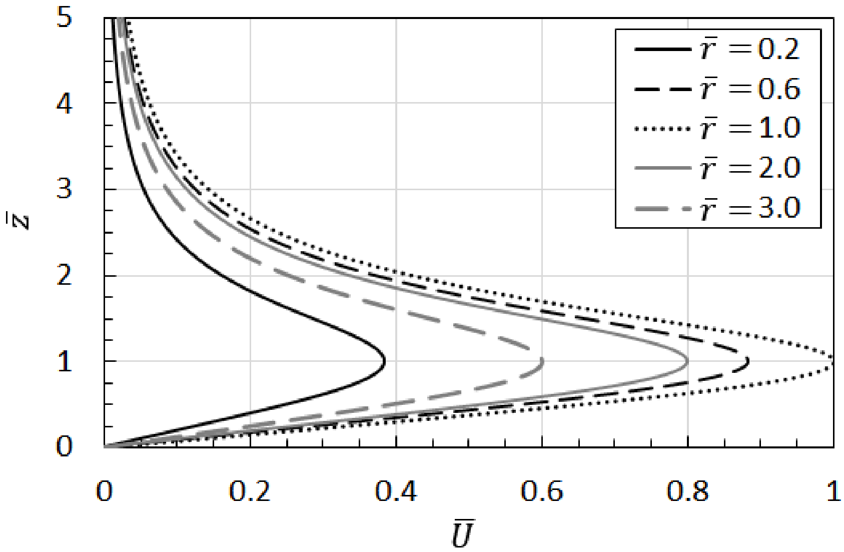


**Figure 2. Radial velocity in downburst**

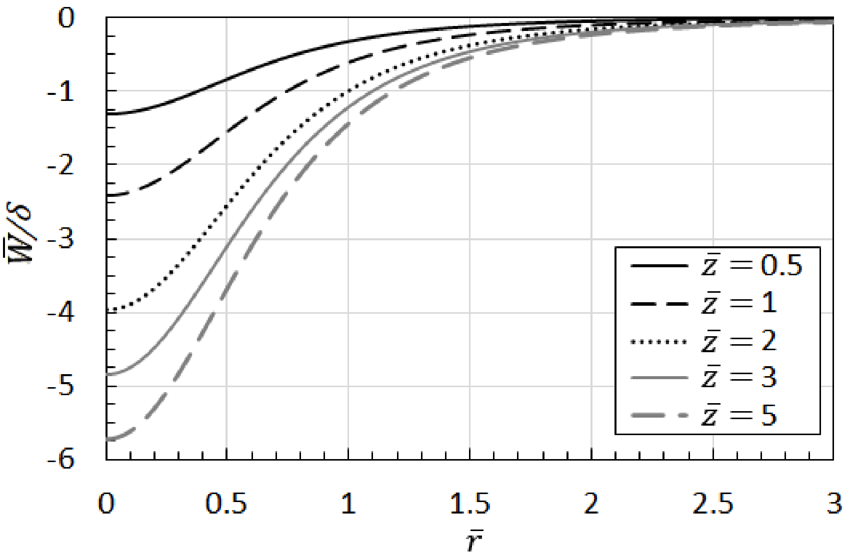


**Figure 3. Vertical velocity in downburst**

## 4. Crop patterns due to a downburst

### 4.1 Calculation of lodging patterns

Whilst the above expressions are of some interest and may have a wider use, in this paper we are primarily interested in the wind conditions near ground level at a height equivalent to the crop's centre of gravity ($z_c$), where the vertical component is small. We thus write the following expression for the radial downburst velocity $U_c$ at crop height

$$\overline{U}_c = \frac{U_c}{U_{mc}} = \frac{2\bar{r}}{(1+\bar{r}^2)} \quad (6)$$

where $U_{mc}$ is the maximum radial velocity at crop height and is given by

$$U_{mc} = U_m \frac{4(z_c/z_m)}{(3+(z_c/z_m)^4)} \quad (7)$$

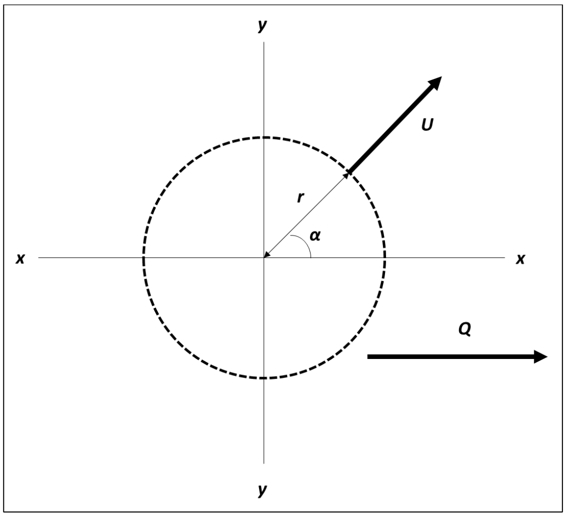


**Figure 4. Co-ordinate system**

In what follows we adopt $U_{mc}$ as our normalization velocity. This can be expected to have values of around 10 m/s, i.e., similar to the lodging values outlined in section 1. The total velocity at crop height at any point $\Omega$ is given by the vector sum of the radial velocity and the translational velocity $Q$, the latter assumed to be in the *x* direction (Figure 4). In normalized terms this is given by

$$\overline{\Omega^2} = (\bar{Q} + \overline{U}_c cos\alpha)^2 + (\overline{U}_c sin\alpha)^2 = \bar{Q}^2 + 2\bar{Q}\overline{U}_c cos\alpha + \overline{U}_c^{\,2} \quad (8)$$

where $\bar{Q} = Q/U_{mc}$ and $\overline{\Omega} = \Omega/U_{mc}$. The translational velocity $Q$ can be expected to be around 1 to 3 m/s (Xhelaj et al., 2020) and thus values of $\bar{Q}$ of 0.1 to 0.3 are appropriate.

(At this point it is worth noting that the analysis that follows does not apply for the stationary downburst case with $\bar{Q} = 0$ for which the flow dynamics are very different. We consider this special case in the Appendix and in particular consider the lower limit of translational velocity for which the analysis that follows is applicable. Additionally, surface roughness (due to varying plant height and local topography) are expected to result in very different flow interaction near ground; however, due to the complexity, were not considered).

The flow angle relative to the *x* axis is given by

$$\theta = tan^{-1}\left(\frac{\bar{U}_c sin\alpha}{\bar{Q}+\bar{U}_c cos\alpha}\right) \qquad (9)$$

Now we are particularly interested in the points in the flow field where the overall velocity is equal to the lodging velocity $\Omega_l$ i.e. the point at which lodging occurs. In normalised terms, the curve along which this occurs is given by substituting $\bar{U}_c$ from equation (6) into equation (8), resulting as follows:

$$\bar{\Omega}_l^{\,2} = \left(\frac{\Omega_l}{U_{mc}}\right)^2 = \bar{Q}^2 + 2\bar{Q}\bar{U}_c cos\alpha + \bar{U}_c^{\,2} = \bar{Q}^2 + 2\bar{Q}\frac{2\bar{x}}{(1+\bar{r}^2)} + \left(\frac{2\bar{r}}{(1+\bar{r}^2)}\right)^2 \qquad (10)$$

where $\bar{r}^2 = \bar{x}^2 + \bar{y}$, $\bar{x} = x/r_m$ and $\bar{y} = y/r_m$. For values of $\bar{\Omega}_l$ below 1.0, the lodging velocity is less than the maximum velocity at crop's centre of gravity in the downburst and thus the downburst alone will cause the crop to lodge. For values above 1.0, the crop will only lodge when there is an added translational velocity of sufficient magnitude.

It is not possible to find a simple expression that gives the curve of equation (10) in simple $x, y$ terms, and a numerical solution is required. Nonetheless the form of this equation suggests that this curve will be defined by two parameters $\bar{\Omega}_l$ and $\bar{Q}$. Typical boundaries illustrating the form of this initial curve are given in Figure 5 below for $\bar{\Omega}_l = 0.8$ and $\bar{Q} = 0.1$ to $0.3$ and for $\bar{Q} = 0.2$ and $\bar{\Omega}_l = 0.6$ to $0.8$. Values of $\bar{\Omega}_l$ below 1.0 implies that the lodging velocity is below the maximum value of the downburst wind velocity and thus regons where lodging occurs can be expected. The figures show a region of the $\bar{x}$ - $\bar{y}$ plane with the downburst centre at the origin. All the curves show an outer black curve that gives the extent over which the wind velocity exceeds the lodging velocity, and the curves for the lower values of $\bar{Q}$ and $\bar{\Omega}_l$ show an inner red curve around the region close to the centre of the downburst where the total velocity is less than the lodging velocity, due to the fact that the downburst velocity falls to zero at the centre. It can be seen that as the translational component of velocity increases, the lodging region increases in extent and is stretched in the $\bar{x}$ direction, and the inner low velocity region disappears. As the lodging velocity increases the extent of the lodging region shrinks as would be expected.

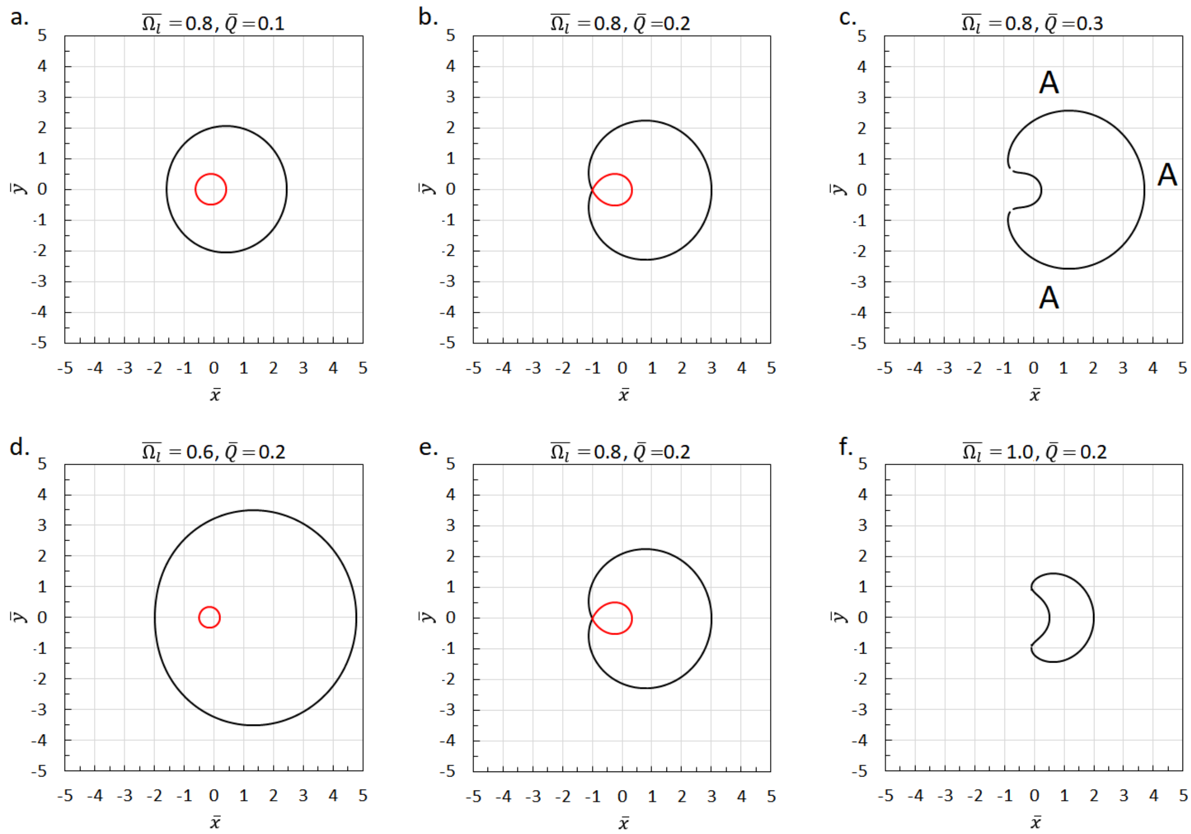


**Figure 5. Regions where the wind velocity initially exceed the lodging velocity (N.B., the downburst (and lodging front) would continue to translate from left to right.)**

Now let us consider the lodging process as a downburst passes over a crop. The crop will lodge at the point where, for any one value of the lateral distance $\bar{y}$, the overall velocity first exceeds the lodging velocity, i.e. the right hand side of the lines given by AAA on Figure 5c. We will refer to this as the lodging front. The lodging front has a dimensionless width of $\bar{Y}$ and is the overall width of the region for which the overall velocity exceeds the lodging velocity at some point as the downburst passes across. The above analysis suggests that $\bar{Y}$ should be a function of $\bar{\Omega}_l$ and $\bar{Q}$. This variation is shown in Figure 6 below for a range of variation of these parameters.

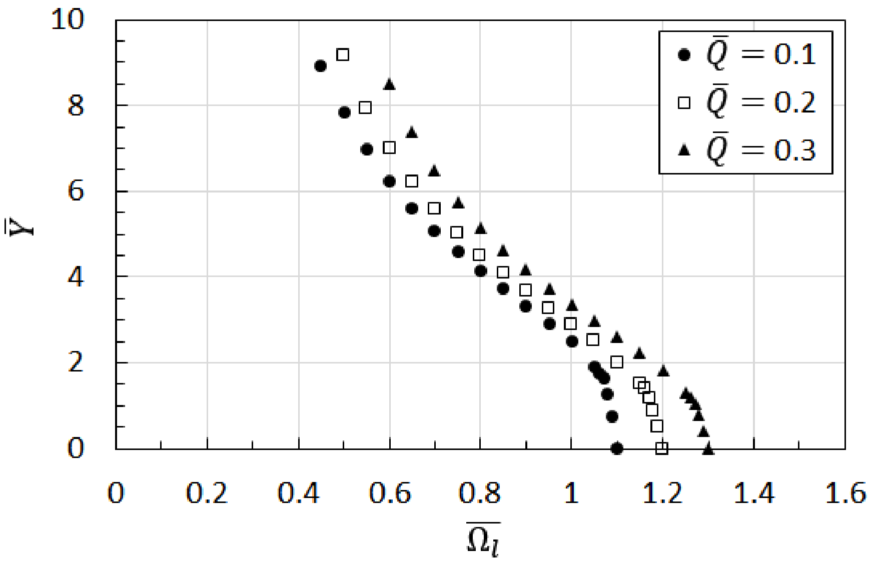


**Figure 6. Variation of the lodging width with $\bar{\Omega}_l$ and $\bar{Q}$**

This figure shows that the lodging width falls as $\bar{\Omega}_l$ increases, i.e. as the crop becomes stronger, but increases as the translational velocity increases $\bar{Q}$, as would be expected. For any value of $\bar{Q}$ the lodging width falls to zero for a value of $\bar{\Omega}_l = 1 + \bar{Q}$. This represents the condition where the sum of the maximum velocity in the downburst and the translational velocity is equal to the lodging velocity for $\bar{Y} = 0$.

The crop will fall in the direction of the lodging velocity on the lodging front, denoted by $\theta$. Figure 7 shows $\theta$ increases from zero at the centre of the lodging front to maximum values Δ of the order of 40 to 70° at the edge of the front. Thus one would expect to see a diverging pattern of crop fall when a downburst passes over a crop.

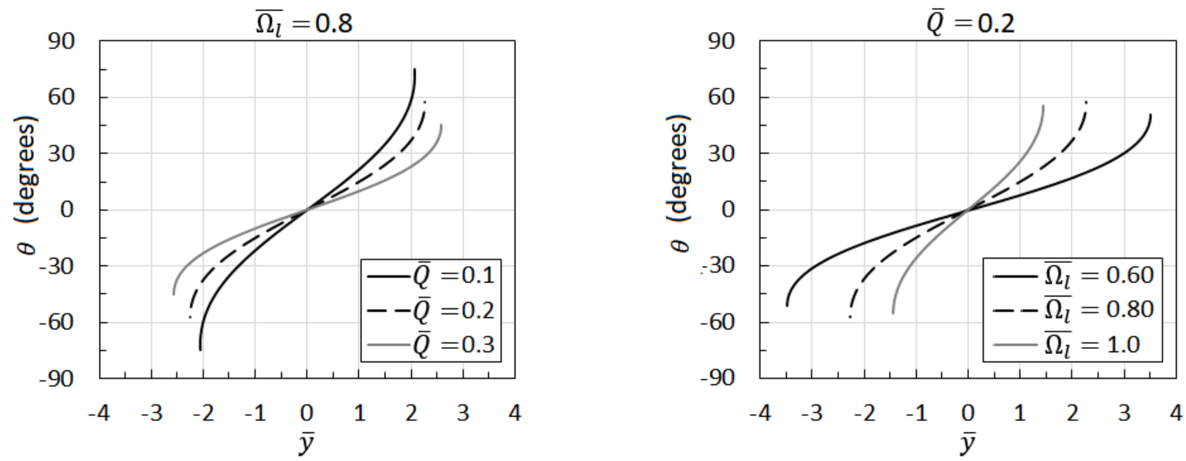


**Figure 7. Variation of lodging angle across the lodging front for $\bar{\Omega}_l$ = 0.8 and a range of values of $\bar{Q}$**

Interestingly, if the values of $\bar{y}$ and $\theta$ in the above figure are normalised with their maximum values $0.5\bar{Y}$ and $\Delta$ for each value of $\bar{Q}$ they collapse onto one curve as can be seen in Figure 8 below. This will be seen to be useful in what follows.

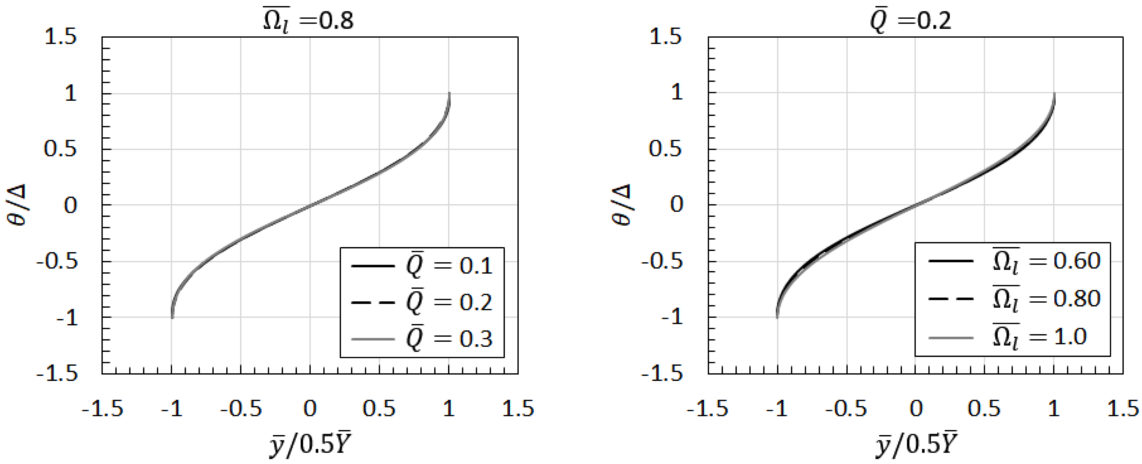


**Figure 8. Renormalisation of lodging angle curve**

Figure 9 shows the angle of fall at the edge of the lodging front $\Delta$ (the maximum value), again as a function of the parameters $\overline{\Omega_l}$ and $\bar{Q}$. This variation is complex, but again the lodging angle tends to zero for $\overline{\Omega_l} = 1 + \bar{Q}$ as would be expected.

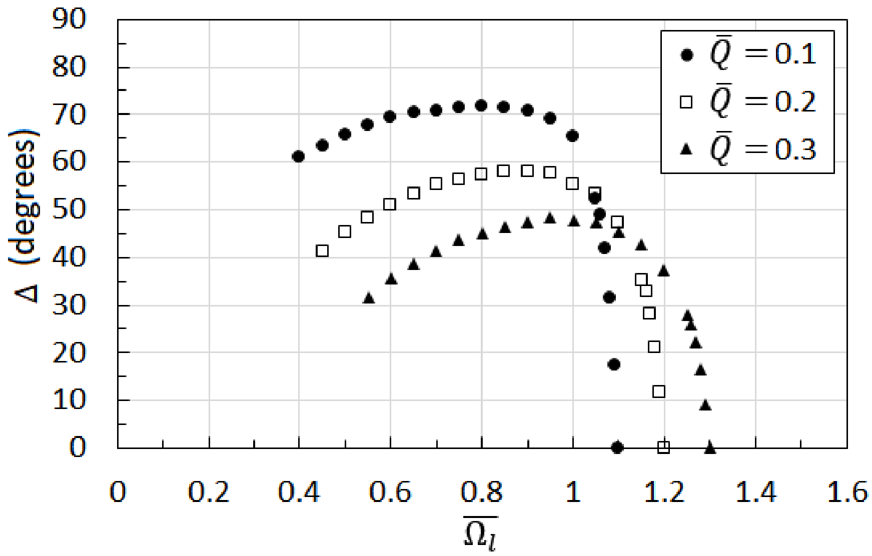


**Figure 9. Variation of maximum lodging angle with $\overline{\Omega_l}$ and $\bar{Q}$**

## 4.2 The effect of crop variability

It was shown in section 1 that crop geometric and strength parameters can vary significantly, and that this variation resulted in a lodging velocity that can have a standard deviation of around 20% of the mean. In this section we consider how this variation in lodging speed can affect crop fall patterns. We adopt the following procedure.

We firstly assume a hypothetical field, 1000m square, divided into 10,000 10m squares. In each square we assume constant plant parameters and thus a constant lodging velocity. For each section of the field a value of normalised lodging velocity is randomly generated, assuming a mean value of $\overline{\Omega}_l$ of 0.8 and standard deviation between 0 and 20% of the mean (with the higher value being in line with the values given in section 1). We then assume that a downburst, with a value of $r_m$ of 100m passes along the centre line of the field (taken as the *x* direction) with a normalised translational velocity $\bar{Q}$ of 0.2. Thus, the edges of the field are at values of $\bar{y}$ of ±10.

For each section of the field, we use the generated values of $\overline{\Omega}_l$ to calculate an equivalent lodging track width $\bar{Y}$ from the curve for $\bar{Q} = 0.2$ of Figure 6 and for the maximum crop fall angle Δ from the curve for $\bar{Q} = 0.2$ of Figure 9. Thus, for each section of the field we have values of $\bar{y}$, $\bar{Y}$ and Δ, and can thus calculate the crop fall angle from the normalised curves of Figure 8. As the values of $\overline{\Omega}_l$ have been generated by a random process, these angles will also show some variability. This is illustrated in the vector plot of Figure 10 for a standard deviation of 20% of the mean and in the sectional plots for one section of the field normal to the downburst translational direction of Figure 11 for a range of standard deviations.

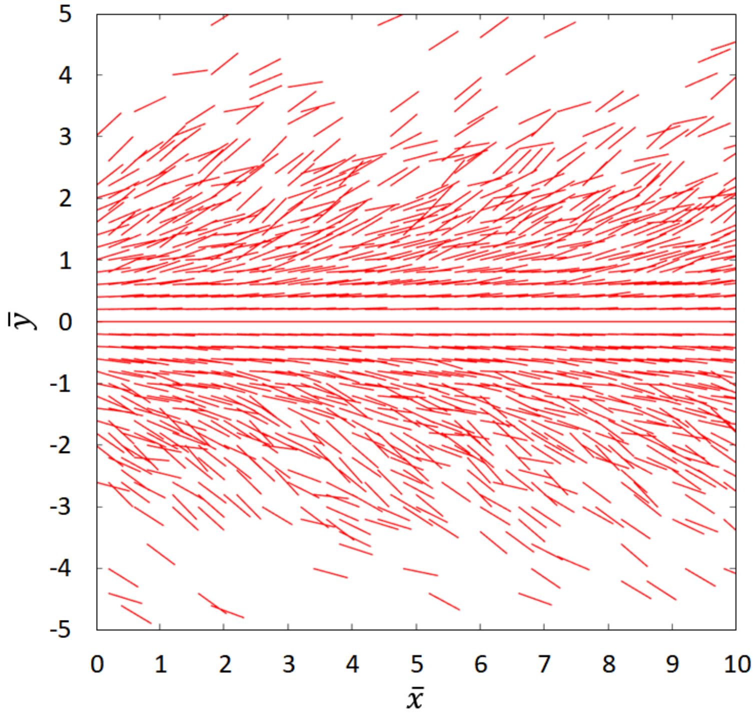


**Figure 10. Vector plot of cropfall directions for a standard deviation of lodging velocity of 20% of the mean.**

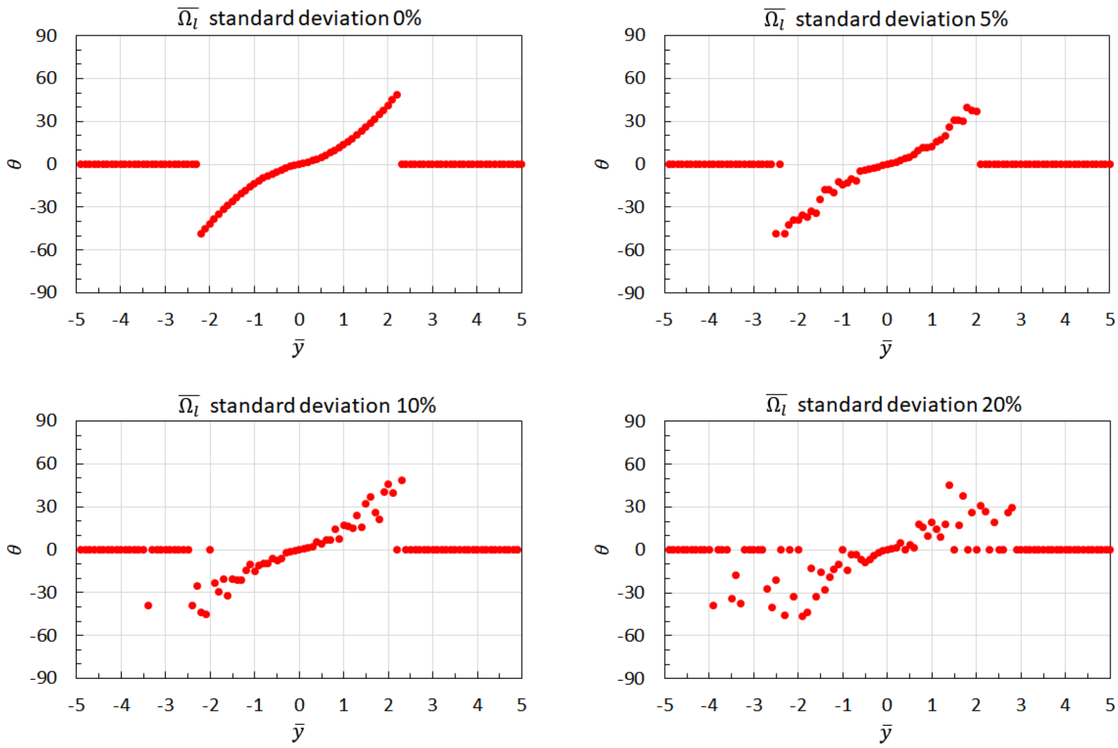


**Figure 11. Crop fall angles across the lodging track for different standard deviations of lodging velocity used in the simulation.**

It can be seen from the latter that there is very considerable variation in crop fall angle for the higher standard deviations of the generated crop fall velocities, particularly towards the edge of the lodging region. This is due to the crop parameter variability that leads to a wide spread of lodging velocities.  That being side the proportion of the crop that lodges only varies slightly – from 56% when the lodging velocity standard deviation is zero to 53% when it has a value of 20% of the mean.

### 4.3 Comparison with field data

(a)

(b)

**Figure 12.** Observed crop fall pattern at a) Eden-Walsh (80.3878 W, 42.7244 N, area 198 x 132 m) and b) Ailsa Craig (81.5645 W, 43.1514 N, area 168 x 112 m) on 12/09/21 (red lines indicating the local cropfall direction). Reproduced with permission form the Northern Tornadoes Project.

Figure 12 shows two aerial photographs of crop fall at Eden-Walsh and Ailsa Craig (Ontario, Canada) on 12/09/21 caused by downbursts. The crop fall directions are indicated by red lines. Note the drawing of these lines is somewhat subjective and should not be regarded as having great accuracy. The Eden-Walsh picture shows a fairly clear divergent crop fall pattern in the lower half of the photograph, as would be expected from the above analysis, albeit with only a relatively small amount of the crop lodged, with a rather more chaotic lodging pattern in the top half of the photograph. Note that it is quite possible that these two patterns were formed by different downbursts at different times. The Ailsa Craig photograph shows lodging across the area that it covers, and again shows a broadly divergent cropfall pattern in line with the analysis.

Unfortunately, crop fall analysis arising from downbursts is at its infancy; there are currently insufficient aerial images of the correct resolution available to undertake a meaningful comparison with the model. Furthermore, local topography inhomogeneities and surface roughness are expected to contribute to turbulence generation, however, have largely been neglected, which may not be the case in reality. Nevertheless, the general agreement (albeit highly subjective) with model results is promising.

### 4.4 Some closing remarks

The model outlined above shows that for downbursts the crop fall pattern is broadly divergent from the centre line of the downburst. This is very different from the lodging patterns caused by the passage of tornadoes – see Baker et al (2020) where there are zones of both convergence and divergence of crop fall direction. Thus, in broad terms, the two models can be used to distinguish between the passage of tornadoes and downbursts over crops.

But is it possible to use the model to identify downburst parameters in a more quantitative way? From Figures 6 and 9, the lodging width and the crop fall angle at the edge of the lodging track can be expressed in the functional forms

$$\frac{Y}{r_m} = fn\left(\frac{\Omega_l}{U_{mc}}, \frac{Q}{U_{mc}}\right) \quad (11)$$

$$\Delta = fn\left(\frac{\Omega_l}{U_{mc}}, \frac{Q}{U_{mc}}\right) \quad (12)$$

In principle, from a specific crop fall pattern, $Y$ and $\Delta$ can be measured, although the photographs shown above suggest that this is not a straightforward task. However, the work undertaken by Lombardo et al. (Rhee et al., 2020) on trees shows that it is possible to automate such tasks given aerial images of a sufficient quality. In addition, the lodging velocity $\Omega_l$ can in principle be calculated from measured plant parameters through equation (1). Again, the work of Berry et al. (2004) has shown that this is relatively straightforward to do. However, even if these measurements are possible, the functional expressions suggest they are not in themselves sufficient for fully determining the parameters of the downburst, as we have only two equations with three unknowns $r_m$, $U_{mc}$ and $Q$. Of these the translational velocity $Q$ is perhaps the one that can most easily be estimated from satellite or aerial observations. If this is the case, then there is a possibility that the downburst parameters $r_m$, and $U_{mc}$ can be estimated from crop fall patterns, but the estimation chain is a long one, with many uncertainties. However, the latter is not uncommon when working with plants!

It is also with nothing that the model employed in this study was assumed to occur in a stationary environment. The interaction between downburst flow and the background atmospheric boundary layer winds can be complex and differs to an isolated downburst flow.

As indicated by the recent works of Moeini and Romanic (2022), this may be an important area which has hitherto largely been neglected.

## 5. Conclusions

This paper has derived and integrated a new model capable of representing the near-surface wind fields with an existing crop model to examine possible crop fall patterns which may arise as a result of a downburst-like event. The following conclusions are drawn:

- Whilst the flow within a downburst like event is spatially complicated, it is possible to represent all three components of the velocity field with a relatively simple model which satisfies the continuity equation.
- It is highly likely that crop fall in downbursts is solely a result of stem failure, given the fatigue like behaviour associated with stem lodging.
- Unlike other synoptic events, crop fall due to downbursts results in a diverging flow pattern.
- The region of crop failure is a function of the local wind speed due to the downburst and its translation speed. This region can be quantified by use of a dimensionless parameter, i.e., the lodging width.
- The angles at which the crops fall depend on their relative location on the lodging front, i.e., the region where the local velocity exceeds the crop lodging velocity. Through suitable normalisation, all lodging angle curves are shown to collapse onto a single lodging curve.
- Crop variability (due to natural factors and/or husbandry treatments) effects not only the impact the angle at which crop fail, but whether the crop actually fails.
- Initial analysis using two full-scale images, suggests that the trends predicted by the model are appropriate.
- Using the model in conjunction with full-scale data, it is possible to calculate a range of downburst parameters which resulted in the observed failure. To obtain a single set of downburst parameters then additional data would be required. The acquisition of this additional data is not uncommon for the analysis of other types of non-synoptic events (e.g., tornadoes). This suggests that the model has utility.

It is recommended that further work is undertaken to ensure that the above analysis could be used in practice to estimate the strength of the downburst, namely:

- The downburst model derived in the paper needs to be validated against an extensive range of full-scale data. Given the transient data of downbursts and the probability that measurement equipment could be appropriately located (both spatially and temporarily) this will be a challenge. However, the work of Solari et al. has shown that such events tend to occur more frequently than what might have been initially suspected.
- More full-scale data similar to that which has started to be routinely collected as part of field campaigns, e.g., The Northern Tornadoes Project in Canada. This data should not only include drone imagery but suitable measurements of the required plant parameters – at the very least, the variety of the crop and associated husbandry treatments should be recorded.

- The approach developed in this paper has the potential to be extended to trees. Noting that fallen trees have the potential to remain in place longer than lodged crops, and their size (compared to crops) ensures that that it is potentially easier to identify the exact angle of tree fall from aerial images, this could offer an opportunity to prove (or otherwise) practicality of this research.

**Appendix – The stationary downburst case**

For the case of a stationary downburst the situation is rather different from that considered in the main body of this paper. There will be essentially only a radial outflow, with the velocity given by equation (6). The crop will thus lodge when the flow velocity exceeds the lodging velocity i.e.

$$\bar{\Omega}_l = \frac{2\bar{r}}{(1+\bar{r}^2)}$$

This equation has two roots

$$\bar{r}_1 = \frac{1-\sqrt{1-\bar{\Omega}_l^{\,2}}}{\bar{\Omega}_l} \qquad \bar{r}_2 = \frac{1+\sqrt{1-\bar{\Omega}_l^{\,2}}}{\bar{\Omega}_l}$$

where $\bar{r}_1 = r_1/r_m$ and $\bar{r}_2 = r_2/r_m$. These correspond to the inner and outer edges of an annular ring. Between these circles the crop will lodge in a radial direction. The thickness of the ring will be given by the difference between the two roots

$$\bar{r}_2 - \bar{r}_1 = \frac{2\sqrt{1-\bar{\Omega}_l^{\,2}}}{\bar{\Omega}_l}$$

Now, whilst the stationary downburst situation is unlikely to occur in reality, its consideration does enable a lower limit to be obtained for the downburst duration for the model outlined in the main text to be valid. Assuming that at low translational velocity the downburst keeps its circular shape, then the model outlined above will become valid once the lodging front has passed over a section of crop. This will occur when

$$\bar{D} = \frac{\bar{r}_2}{\bar{Q}}$$

where $\bar{D} = \frac{DU_m}{r_m}$ and *D* is the downburst duration. Thus

$$\bar{D} = \frac{1+\sqrt{1-\bar{\Omega}_l^{\,2}}}{\bar{Q}\bar{\Omega}_l}$$

For typical values of $\bar{Q}$ and $\bar{\Omega}_l$, $\bar{D}$ has values between 5 and 20, and thus for $r_m = 100m$ and $U_m = 10m/s$, the minimum down burst duration for the validity of the theoretical approach will be between 50 and 200s – of the order of 1 to 3 minutes.

## CRediT authorship contribution statement

**Mark Sterling:** Formal analysis, Metholodgy, Writing – original draft, Writing – review & editing**.** **Shen (Ryan) Shuan Huo:** Software, Visualization, Writing – original draft, Writing – review & editing. **Chris Baker:** Formal analysis, Methodology, Writing – original draft, Writing – review & editing.

## Declaration of Competing Interests

The authors declare that they have no know competing financial interests or personal relations that could have appeared to interest the work reported in this paper.

## Acknowledgements

The photograph used in Figure 12 were kindly provided by Greg Kopp and Aaron Jaffe from University of Western Ontario and were recorded as part of the Northern Tornadoes Project. Their help is gratefully acknowledged.

## Funding sources

This research did not receive any specific grant from funding agencies in the public, commercial, or not-for-profit sector. However, its origins can be traced back tornado related research on the Northern Tornadoes Project for which funding was received.

## References


Abd–Elaal, E.S., Mills, J.E., Ma, X., (2013). An analytical model for simulating steady- state flows of downburst. *Journal of Wind Engineering and Industrial Aerodynamics,* 115:53–64.

Aboshosha, H., Bitusamlak, G and El Damatty, A. (2015). Turbulence characterization of downbursts using LES. *Journal of Wind Engineering and Industrial Aerodynamics,* Vol. 135, 44-61. https://doi.org/10.1016/j.jweia.2014.10.020

ASCE 49-21 (2022) Wind Tunnel Testing for Buildings and Other Structures. SBN 9780784483367

Babaei, R., Graat, K., Chan, C., and Savory, E (2021) Experimental simulation of stationary and travelling density-driven thunderstorm down burst using the two fluid model. *Journal of Wind Engineering and Industrial Aerodynamics.* Vol. 211, 104553. https://doi.org/10.1016/j.jweia.2021.104553

Baker, C. J and Sterling, M (2017) Modelling wind field and debris flight in tornadoes. *Journal of wind Engineering and Industrial Aerodynamics*. 168, 312-321.

Baker, C. J, Sterling, M and Jesson M (2020) The lodging of crops by tornadoes. *Journal of Theoretical Biology.* https://doi.org/10.1016/j.jtbi.2020.110309.

Baker, C. J., Sterling, M., and Berry (2014). A generalized model of crop lodging. *Journal of Theoretical Biology*. 363, 1-12. http://dx.doi.org/10.1016/j.jtbi.2014.07.032.

Baker, C. J. and Sterling, M (2019). Are tornado vortex generators fit for purpose? *Journal of Wind Engineering and Industrial Aerodynamics.* Vol. 190, 287-292. https://doi.org/10.1016/j.jweia.2019.05.011.

Berry, P. M (2022) Private communication.

Berry, P. M., Sterling, M., Baker, C. J., Spink, J. H., and Sparkes, D. L. (2003). A calibrated model of wheat lodging compared with field measurements. *Journal of Agricultural and Forest Meteorology*. Vol. 119, Issues 3 –4, 167 – 180.

Berry, P.M., Griffin, J.M., Sylvester-Bradley, R., Scott, R.K., Spink, J.H., Baker, C.J., Clare, R.W. (2000) Controlling plant form through husbandry to minimise lodging in wheat, *Field Crops Research*, Vol 67, Issue 1, 2000, 59-81, https://doi.org/10.1016/S0378-4290(00)00084-8.

Berry, P. M., Sterling, M., Spink, J. H., Baker, C. J., Sylvester-Bradley, R., Mooney, S. J., Tams, A. R., and Ennos, A. R. (2004) Understanding and reducing lodging in cereals. *Advances in Agronomy*. Vol. 84. 215-269.

Berry, P.M., Baker, C.J., Hatley, D., Dong, R., Wang, X., Blackburn, G.A., Miao, Y., Sterling, M and Whyatt, D. (2020) Development and application of a model for calculating the risk of stem and root lodging in maize. *Field Crops Research.* https://doi.org/10.1016/j.fcr.2020.108037.

Burlando, M., Zhang, S. and Solari, G (2018) Monitoring, cataloguing, and weather scenarios of thunderstorm outflows in the northern Mediterranean *Natural Hazards and Earth System Sciences*, 18, 2309-2330, 10.5194/nhess-18-2309-2018

Canepa, F., Burlando, M and Solari, G (2020) Vertical profile characteristics of thunderstorm outflows. *Journal of Wind Engineering and Industrial Aerodynamics.* 104332. https://doi.org/10.1016/j.jweia.2020.104332

Chay, M.T., Albermani, F., Wilson, R., (2006) Numerical and analytical simulation of downburst wind loads. *Engineering Structures*, 28(2): 240-254.

Chay, M.T., Letchford, C.W., (2002a) Pressure distributions on a cube in a simulated thunderstorm downburst—Part A: stationary downburst observations. *Journal of Wind Engineering and Industrial Aerodynamics*. 90, 711–732.

Chay, M.T., Letchford, C.W., (2002b) Pressure distributions on a cube in a simulated thunderstorm downburst—Part B: moving downburst observations. *Journal of Wind Engineering and Industrial Aerodynamics*. 90, 733–753.

Fujita, T.T., (1981). Tornadoes and downbursts in the context of generalized planetary scales. *Journal of Atmospheric Sciences* 38, 1511–1534.

Hjelmet, M. R. (1988) Structure and life cycle of microburst outflows observed in Colorado. *Journal of Applied Meteorology*, 27, 900-927. August.

Holmes, J.D., and Oliver, S.E., (2000). An empirical model of a downburst. *Engineering Structures*, 22(9):1167-1172

Ivan, M., (1986). A Ring-Vortex Downburst Model for Flight Simulations. *Journal of Aircraft*, 23(3), 232-236

Jesson, M and Sterling, M (2017) A simple vortex model of a thunderstorm downburst – a parametric investigation. *Journal of Wind Engineering and Industrial Aerodynamics*. Vol. 174, 1-9. https://doi.org/10.1016/j.jweia.2017.12.001

Jesson, M., Sterling, M., Letchford, C and Haines, M (2015) Aerodynamic forces on generic buildings subject to transient downburst-type winds. *Journal of Wind Engineering and Industrial Aerodynamics.* 137, 58-68

Jesson, M., Lombardo, F. T., Sterling, M and Baker, C. J (2019) The physical simulation of a transient downburst-like event – how complex does it need to be? *Journal of Wind Engineering and Industrial Aerodynamics.* 189, 135-150.

Joseph., G., Mohammadi, M., Sterling, M., Baker, C. J., Berry, P. M., Hatley, D., Blackburn, A., Whyatt, D, Murray, J., Gullick, D., and Finnan, J. (2020). Determination of crop dynamic and aerodynamic parameters for lodging prediction. *Journal of Wind Engineering and Industrial Aerodynamics.* https://doi.org/10.1016/j.jweia.2020.104169

Kim, J., Hangan, H., (2007) Numerical simulations of impinging jets with application to downbursts. *Journal of Wind Engineering and Industrial Aerodynamics*. 95, 279–298.

Lombardo, F., Roueche, D and Prevatt, D (2015) Comparison of two methods of near-surface wind speed estimation in the 22 May, 2011 Joplin, Missouri Tornado. *Journal of Wind Engineering and Industrial Aerodynamics*. 138, 87-97. https://doi.org/10.1016/j.jweia.2014.12.007

Li, C., Li., Q. S., Xiao, Y.Q and Ou, J. P (2012) A revised empirical model and CFD simulations for 3D axisymmetric steady-state flows of downburst and impinging jets. *Journal of Wind Engineering and Industrial Aerodynamics*. Vol. 102. 48-60.

Mason, M.S., James, D.L., Letchford, C.W., (2009) Wind pressure measurements on a cube subjected to pulsed impinging jet flow. *Wind and Structures*. 12, 77–88. https://doi.org/10.1016/j.jweia.2011.12.004

McConville, A. C., Sterling, M and Baker, C. J (2009) The physical simulation of thunderstorm downdrafts. *Wind and Structures*. Vol. 12, No. 2, 133-149.

Moeini, M., & Romanic, D. (2023). An Analytical Solution to the Perturbation Analysis of the Interaction between Downburst Outflows and Atmospheric Boundary Layer Winds, Journal of the Atmospheric Sciences, 80(1), 301-319. doi: https://doi.org/10.1175/JAS-D-22-0123.1

Mohammadi, R., Finnan, J., Sterling, M., and Baker C. J., (2020) A calibrated oat lodging model compared with agronomic measurements. *Field Crops Research*. 225 107784. https://doi.org.10.1016/j.fcr.2020.107784.

Rhee, D., and Lombardo, F (2018) Improved near-surface wind speed characterization using damage patterns. *Journal of Wind Engineering and Industrial Aerodynamics.* 180, 288-297. https://doi.org/10.1016/j.jweia.2018.07.017

Rhee, D., Lombardo, F and Kadowaki (2020) Semi-automated tree-fall pattern identification using image processing technique: Application to alonsa, MB tornado. *Journal of Wind Engineering and Industrial Aerodynamics.* 208, 104399. https://doi.org/10.1016/j.jweia.2020.104399

Romanic, D., and Hangan, H (2020) Experimental investigation of the interaction between near-surface atmospheric boundary layer wind and downburst outflow. *Journal of Wind Engineering and Industrial Aerodynamics*. Vol. 205, 104343. https://doi.org/10.1016/j.jweia.2020.104323

Romanic, D., Nicolini, E.M., Hangan, H, Burlando, M., and Solari, G (2020) A novel approach to scaling experimentally produced downburst-like impinging jet outflows. *Journal of Wind Engineering and Industrial Aerodynamics.* Vol. 196, 104025,

Sterling, M., Baker, C. J., Berry, P. M., and Wade, A. (2003). An experimental investigation of the lodging of wheat. *Journal of Agricultural and Forest Meteorology*. Vol. 119, Issues 3 –4, 149 – 165.

Solari, G., Burlando, M., De Gaetano, P. and Repetto, M. P Characteristics of thunderstorms relevant to the wind loading of structures (2015a). *Wind and Structures*, 20, 763-

Solari, G., De Gaetano, P and Repetto, M. P (2015b) Thunderstorm response spectrum: fundamentals and case study. *Journal of Wind Engineering and Industrial Aerodynamics.* 143, 62-77, 10.1016/j.jweia.2015.04.009

Solari, G., Burlando, M., and Repetto, M.P. (2020) Detection, simulation, modelling and loading of thunderstorm outflows to design wind-safer and cost-efficient structures *Journal of Wind Engineering and Industrial Aerodynamics.* 200, 104142, 10.1016/j.jweia.2020.104142

Xhelaj, A., Bulando, M and Solari, G (2020) A general-purpose analytical model for reconstructing the thunderstorm outflows of travelling downbursts immersed in ABL flows. *Journal of Wind Engineering and Industrial Aerodynamics*, 207, 104373.